

PACKING ANALYSIS IN REACTIVE CRYSTALS: THE DECOMPOSITION OF
BIS(3,3,3-TRIPHENYLPROPANOYL) PEROXIDE IN THE SOLID STATE

A. GAVEZZOTTI

Dipartimento di Chimica Fisica ed Elettrochimica e Centro CNR,
Università di Milano, via Golgi 19, 20133 Milano (Italy)

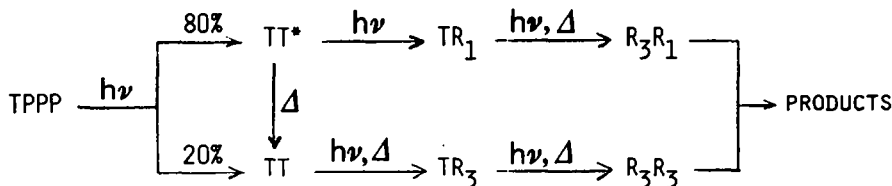
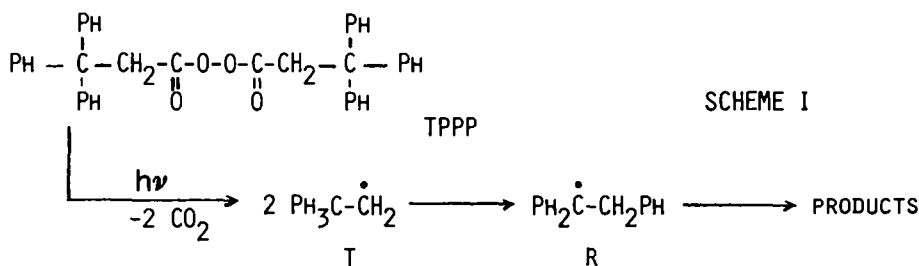
(Received in UK 16 February 1987)

Abstract - Crystal potential energy calculations and packing analysis are presented for the title reaction, a solid-state process which has been carefully studied by McBride and coworkers by EPR and X-ray diffraction. The position of the carbon dioxide molecules resulting from the decomposition was approximately determined by an analysis of the free volume in the crystal and by packing energy calculations.

The subject of organic solid state reactivity is a fascinating one, and reviews dealing with the experimental¹⁻⁴ and theoretical⁵⁻⁶ methods have been given. We have been pursuing in recent years the aim of finding suitable theoretical approaches to the problem, leaning rather on the side of simple arguments based on molecular shape than on rigorous quantum mechanical methods. The fundamental assumption is that the largest part of (or, for some crystals, all of) the intermolecular effects can be rationalized by extending to the solid state the concept of the steric factor, which has proved so successful in the discussion of molecular conformation in the gas phase. Thus, our calculations mainly rely on simple quantifiers of molecular shape and size, like non-bonded intermolecular potentials. The essentials of this way of thinking go back to the works of Kitaigorodski and his school⁷, but we feel that a revival of these ideas is both timely and useful.

This paper describes to some extent the methodologies we have developed, and their application to the solid-state decomposition of the title compound (TPPP henceforth)⁸⁻⁹. A previous application of the same approach to a similar reaction in crystalline diacylperoxides has been described¹⁰.

The overall reaction sequence for the decomposition and subsequent neophyl rearrangement of TPPP is shown in Scheme I, while the solid-state sequence is detailed in Scheme II⁸. In this last Scheme, the radical pairs are named according to their constituent radicals; the subscript of R denotes which of the three phenyl groups migrates, the labelling being possible due to the different crystal environments; and the asterisk denotes strain (it was not ascertained whether intra- or intermolecular) which is relaxed in TT.



SCHEME II

The six radicals have been identified on the basis of EPR spectra from single crystals, and activation energies for each step in Scheme II were obtained⁸. The crystal structure of the starting material (with two solvate benzene molecules per TPPP molecule) was determined⁹, and this was the basis of our analysis. The structure and orientation of the radicals was revealed⁹, but the position of the CO₂ molecules resulting from decarboxylation was only guessed at. This is a very important point, since pressure from the developing CO₂ can steer the reaction to otherwise unfavorable paths³.

Outline of the computational methods

A number of computational techniques for the simulation of the static and dynamic properties of molecular crystals has been proposed and used in our laboratory. Since the description of these techniques is somewhat scattered in different journals, we take this opportunity to collect them in the same place, also because the calculations we report for TPPP are an illustration of their combined use. All the techniques described in the following are embodied in program OPEC¹¹, by now rather widely distributed among crystallographers and organic solid state scientists.

a) crystallographic data

The starting point for our analysis is invariably the X-ray crystal structure of a compound, in the form of cell parameters, space group and atomic coordinates. The coordinates for hydrogen atoms are recalculated for a C-H distance of 1.08 Å and regular CCH angles (i.e. as close as possible to 109.5 or 120°). When avail-

able, thermal parameters (U_{ij}) are sometimes useful, but present-day trends in publication policies very seldom make this information available in the current issues of the journals.

b) basic crystal properties

Among these we list molecular volume (V_m), and molecular surface (S_m), computed according to procedures to be found in refs. 11 and 12, based on molecular geometry, atomic van der Waals radii, and spheres-and-caps or point by point integration methods. From these quantities, the packing coefficient, C_K , can be computed as

$$C_K = Z V_m / V_C, \quad (1)$$

where Z is the number of molecules in a cell of volume V_C . Molecular volumes and surfaces can be broken down into contributions from single atoms, V_{mi} and S_{mi} .

Another important crystal property is the packing potential energy, PPE, defined as the potential energy of one mole of molecules brought from infinity into the crystal; the packing energy, PE, is one half of PPE. When the asymmetric unit is one single molecule, PPE can be computed as:

$$PPE = \sum_i \sum_{k_j} A \exp(-B R_{i,k_j}) - C R_{i,k_j}^{-6} \quad (2)$$

where A , B and C are parameters to be found in the literature for each kind of interatomic contact, i and k run over the atoms in the molecule, and j runs over the molecules which surround the central one in the crystal. The PPE can be broken into molecule-to-molecule terms or even atom-by-atom contributions for the central molecule. The first terms tell for instance which of the surrounding molecules belong to the first, second, third coordination sphere around the central molecule; atom-by-atom contributions may be called atomic relevances, since they tell how much of the total PPE is ascribable to each atom in the molecule. By statistical approaches, average values have been derived for PPE as a function of S_m or V_m ^{11,12}, and average group increments for the calculation of V_m and S_m were given. Deviations of the actual S_m values from the average have been correlated to intramolecular steric effects. Average values for the atomic relevances in crystals for each atomic species have also been obtained¹³, and deviations from the average have been correlated with the position of the atom in the molecule.

The concept of radial distribution of the PPE has also been introduced¹⁴. This is roughly evaluated as follows. Let $E(R)$ be the PPE due to a given atom, as a function of the radial distance from it; this is obtained by breaking down the atomic relevance into contributions from spherical shells around the atom. The first derivative of $E(R)$ is the gradient of the intermolecular potential at that atom, or intermolecular "pressure" (although it has the dimensions of a force). A high atomic relevance and gradient of the radial distribution pertain to atoms which are exposed, or on the rim of the molecule. Low values pertain to atoms which are shielded from the intermolecular field.

When the asymmetric unit does not coincide with one and only one molecular entity (as is the case when there are solvate molecules) the PPE is made up of

many contributions, one for the overall lattice energy of the array of molecular aggregates, and as many as needed to account for the interactions between fragments in the aggregate. Figure 1 gives a pictorial description of this. The equation for PPE becomes

$$\text{PPE} = \text{PPE}(\text{lattice, aggregate}) + 2 \sum_{i>j} E(\text{fragment } i, \text{ fragment } j) \quad (3)$$

and the relationship $\text{PE} = 1/2 \text{PPE}$ still holds. Incidentally, it may be noted that PE is the right quantity to compare with experimental sublimation energies; ref. 5 can be consulted on the uses of these two quantities.

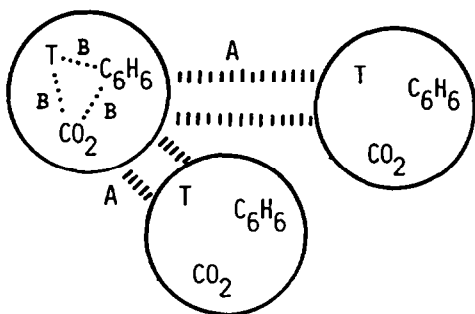


Figure 1. Contributions to the PPE of a molecular aggregate. Contacts A make up $\text{PPE}(\text{lattice, aggregate})$, contacts B are the $E(\text{fragment } i, \text{ fragment } j)$.

c) molecular motions in the crystal

If a molecule or a fragment rotates or translates in the crystal, the PPE changes along the displacement coordinate can be easily calculated by eq. (2) or (3). Many examples of such calculations are available^{5,15-19}. They amount to computing the energy of a guest (the rotated or translated molecule) in the undistorted lattice of the original molecule. Note that this is different from computing the packing energy of a crystal made entirely of displaced molecules - in this case one is dealing with a different crystal structure for the compound. Crystal symmetry is broken in the first case, and preserved in the second.

d) packing analysis by volume analysis

The overall packing coefficient C_K gives very little information as to the chances of molecular motion or reactivity in a crystal. Only global conclusions on tight or loose packing can be drawn from it. The packing coefficient can also be computed in volumes smaller than the whole cell (either slabs or zones); eventually, the packing density can be computed in very small volumes, typically $0.2-0.5 \text{ \AA}^3$, all over the cell, thus giving a packing density map. This is done by a point-by-point integration technique¹¹. In this way, any sort of local inhomogeneities in the crystal, like holes or channels, can be spotted, and their volumes can be calculated by simply summing over partial occupancies of volumes within the boundaries of the hole. While this procedure retains a quite subjective flavor (hole boundaries depend to some extent on the attitude of the observer), it allows an unequivocal identification of discontinuities in close packing, which can be correlated to mobility and reactivity in the crystal. The results of a fair appli-

cation of this procedure are also insensitive to the choice of van der Waals radii since the cross section of significant cavities (typically 2 \AA or more) is one order of magnitude larger than variations in atomic radii available in the literature.

PPE calculations and the volume analysis method show a good amount of synergism, in the sense that they support and complement each other. A molecular movement towards a cavity will show a small PPE activation barrier. Finally, it is worth reminding here that all our calculations concern only intermolecular effects, while the intramolecular ones should be calculated by applicable quantum chemical or molecular mechanics methods²⁰.

Results of the calculations

a) preliminary analysis of the TPPP crystal packing

TPPP crystallizes with two solvate benzene molecules per formula unit. The shape of the molecule is irregular, with two bulky triphenylethyl groups bound through the peroxide linkage. The packing around the oxygens is loose, and a hint to this is provided by the elongated shape of the thermal libration ellipsoids of the peroxide oxygens. Whether they represent a true libration or some sort of disorder cannot be ascertained by either diffraction or theoretical methods.

Table 1. Lattice parameters and other crystal data for TPPP. Average values (see text) in parentheses.

Space group	$\bar{P}1$, Z=1	
Cell volume	1057.9 \AA^3	
Molecular volume	732 \AA^3	
Molecular surface	828 \AA^2 (897)	
Packing coefficient	0.692 (0.704)	
Packing energy (7 \AA cutoff)	60.4 Kcal/mole (64.9)	
Atomic relevances		
Atom	TPPP	DBP ^{a)}
O(carbonyl)	0.52	0.75
O(peroxide)	0.55	0.96
		(0.90)

a) In dibenzoylperoxide; see J.M.McBride and M.W.Vary, Tetrahedron 38,765(1982).

The overall packing coefficient for TPPP (see Table 1) is rather low, but it is not an unusual value for a molecule with irregular shape. The packing energy is also lower than predicted for a compound of its molecular surface. More revealing is the packing coefficient computed in a xy cell slab 0.05 (fractional) thick along z, centered at z=0; this goes down to 0.57, showing the presence of hollows in that zone. Furthermore, the atomic relevances (Table 1) and PPE radial distributions (Figure 2) for the oxygen atoms reveal that they are secluded from the influence of the crystal field, or, conversely, that their displacements will affect but scarcely the potential energy of the crystal.

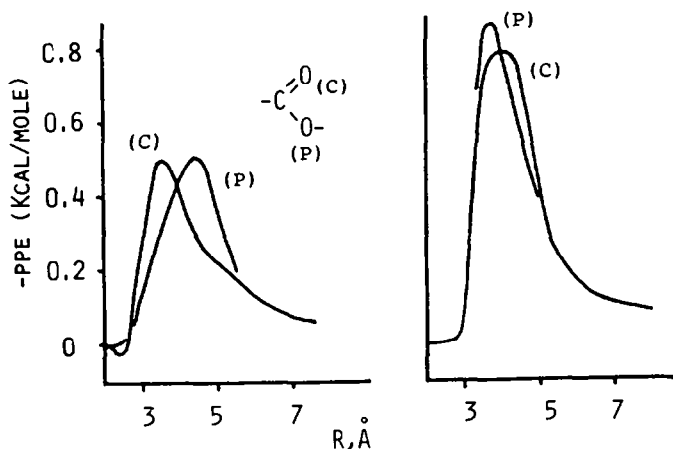


Figure 2. Radial distribution of PPE for oxygen atoms in carbonyl and peroxide oxygen in (left) TPPP and (right) dibenzoylperoxide. Oxygens in TPPP are shielded from contacts in the 3-5 Å range.

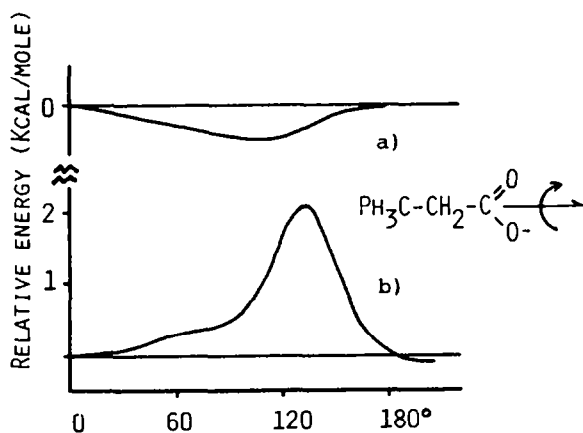


Figure 3. PPE curve for $-\text{COO}$ group rotation around the $\text{C}(1)-\text{C}(2)$ axis (shown). a) PPE between TPPP and the benzene solvate molecules, b) lattice PPE. See eq. (3).

More information on the intermolecular field in the surroundings of the reactive peroxide group can be obtained by calculating the PPE for some specific molecular motions. The first such calculation refers to rotation of the oxygen atoms around the $\text{C}(1)-\text{C}(2)$ axis (Figure 3); this rotation is intermolecularly quite free, the barrier being lower than 1.5 Kcal/mole. Even the rotation of one whole benzene solvate molecule in its plane is almost free, the barrier (Figure 4) being less than 2 Kcal/mole, to be compared with a barrier of about 3 Kcal/mole for the benzene crystal itself¹⁸.

As a result of these preliminary investigations, it can be said that a certain freedom of molecular motion is evident in the TPPP crystal, and that the oxygen atoms are located in a cavity which is partially shielded from the intermolecular field. A more quantitative assessment of these effects is given in the following.

b) analysis of the reaction path for decarboxylation

The first step in the solid-state reactions of TPPP is double decarboxylation and formation of a radical pair (Scheme II). Since CO_2 carries no net spin, its location can be determined only by potential energy calculations.

A full packing density map was calculated for TPPP in its unreacted, ordered

state. The section at $z=0$ of this map is shown in Figure 5: note that the center of symmetry (and the cell origin) coincides with the O-O bond midpoint. The map shows, as expected, large cavities; the one labelled A is about 4 Å wide in the xy section, and its volume is about 9 Å^3 . The volume increment for the decarboxylation reaction can be obtained from the difference in atomic volumes, V_{mi} , for the relevant atoms in the reactant and the products, and is equal to 9.8 Å^3 per CO_2 molecule (it may be even less if, as seems probable, the CO_2 and the radicals are squeezed together to some extent). Thus, cavity A seems at first sight an attractive possibility for the location of CO_2 molecules, which could occupy one cavity each, in neighbouring cells (see arrows in Figure 5). In fact, however, it is not very thick in the z direction, and to avoid mutual repulsion the two CO_2 molecules should travel a long distance, to the center of this cavity. Therefore, no further effort to optimize the CO_2 position in these cavities was attempted.

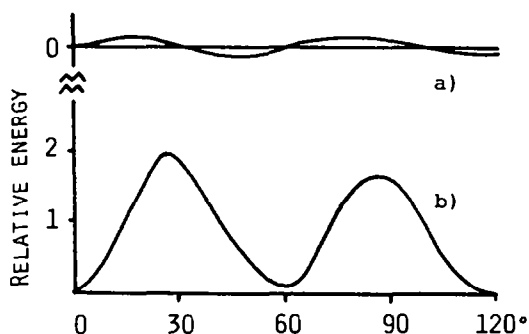


Figure 4. PPE curve for rotation of one benzene solvate molecule in its molecular plane. a) and b) as in Figure 3. kcal/mole units.

The section at $z = -0.10$ (Figure 6) reveals some promising features. Cavity B is level with the C atom of the incipient CO_2 molecule, and roughly midway between the two oxygen atoms in the z direction. It was therefore chosen as a good place to accommodate the excess volume after decarboxylation. In the upper part of Figure 6 is drawn the shape of the CO_2 molecule in its optimized position, it being understood that a centrosymmetrical molecule occupies the same cavity at $z = +0.10$. At the same time, cavity C seems strategically located to accommodate the CH_2 group as it backs off under pressure from CO_2 . An account of how the final position of the CO_2 molecules was found follows.

A model for CO_2 was set up (rigid, $\text{C}=\text{O} \ 1.16 \text{ Å}$), and its center of mass was located about midway between the original C(1) position and the cell origin (but with $z = -0.10$). The CH_2 group was kept in its original position, halfway between tetrahedral and planar. One CO_2 molecule was then rotated around its inertial axes in steps, and the best arrangement was used, after restoring the center of symmetry, as the starting point for a new optimization cycle in which simultaneous rotation of the two CO_2 molecules around an axis joining the C atoms was allowed. Subsequently, also rotations around two cartesian axes perpendicular to that axis were tested. These last rotations were effective in bringing down the T- CO_2 repulsion, but, since the two CO_2 molecules were rotated together, could not reduce their mutual repulsion. At this stage, further displacements of the center of

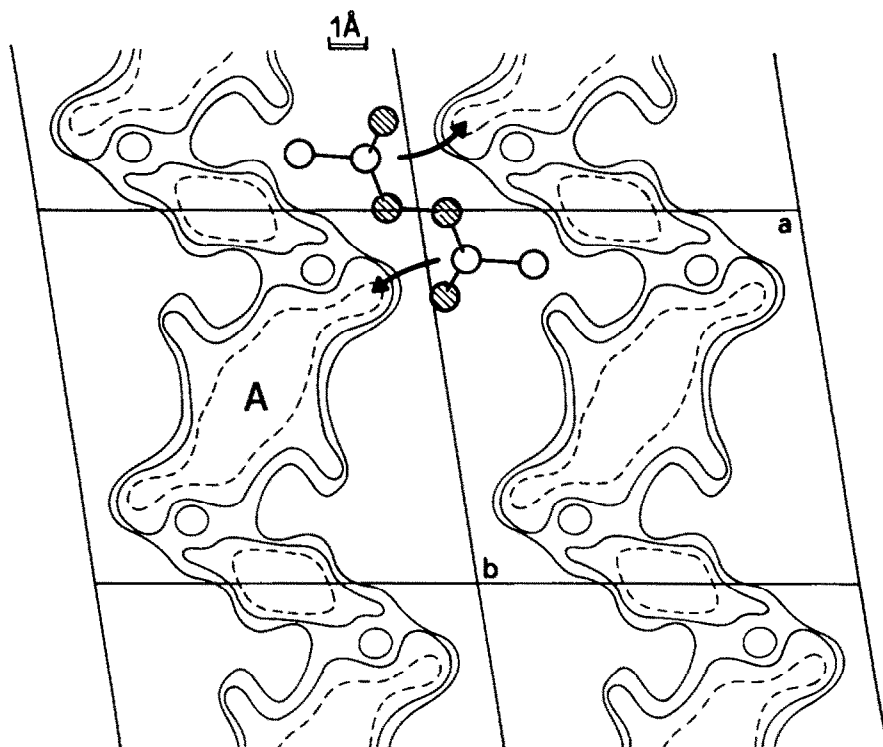


Figure 5. Packing density map for TPPP (xy section at $z=0$; elementary volume 0.12 cube angstroms; isodensity curves from zero-dotted- to 0.4 in steps of 0.2). The C-COO-OOC-C group is shown (oxygens are dashed). The arrows indicate one possible, but probably unfavorable, displacement for the carbon dioxide molecules after reaction.

mass of CO_2 were attempted. Displacements in the xy plane were unfavorable, since they decreased the CO_2 - CO_2 repulsion but increased the T- CO_2 one. A good solution was finally found in a displacement of 0.01 fractional in the z direction. The final energies of interaction among the fragments and the final lattice energies are given in Table 2. Note that these are the potential energies of a guest $2\text{T} + 2\text{CO}_2$ unit in the undistorted TPPP lattice, while the PE change between TPPP and a crystal made of reacted molecules has an upper limit value of 14 Kcal/mole; this means that there may be a chance of obtaining crystals with sizeable reacted domains, on which an X-ray analysis could reveal the position of CO_2 .

Figure 7 shows the van der Waals envelopes of the final sandwich of CO_2 between the T radicals. An activation energy (intermolecular) for reaching this structure of 18 Kcal/mole is calculated. This is just an upper limit value, since optimization of the position of all fragments was not carried to the last; fine adjustments involving small displacements of the CH_2 groups, or of the surrounding or solvate molecules, or slight rotation of the CO_2 molecules away from parallelism, are well beyond the accuracy of our methods. We believe we have brought out very clearly the gross molecular positions after decarboxylation, but when it comes to

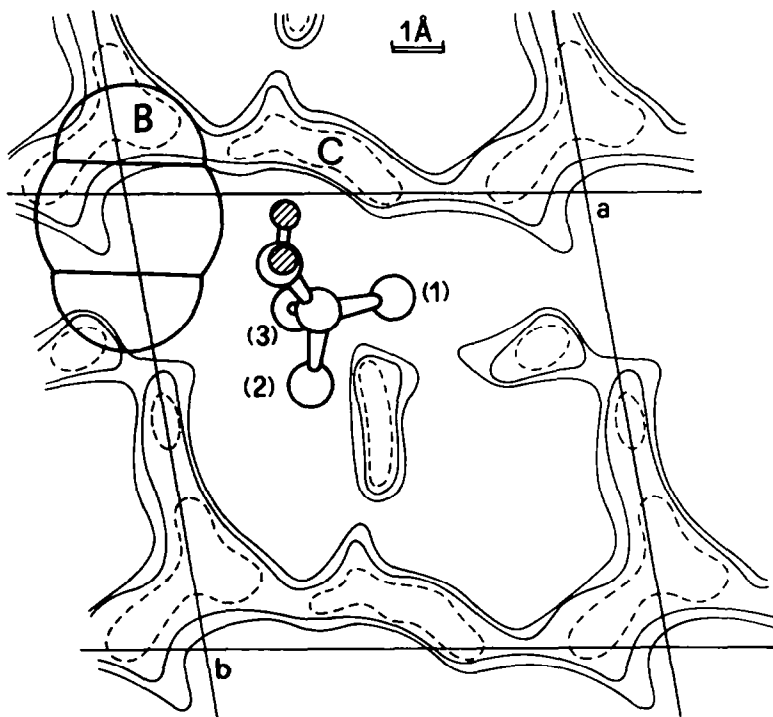


Figure 6. Packing density map for TPPP at $z = -0.10$ (fractional; see also captions to Figure 5). The final position of the CH_2 fragment and of the carbon dioxide molecule are shown. Large spheres are van der Waals envelopes. The phenyl rings are labelled (1), (2), (3), after ref. 9.

the simultaneous effect of many small displacements, the number of variables is so high that a full treatment of the dynamics of the system becomes impossible.

Discussion

Using the information in Figures 5-7, we can now discuss the outcome of our calculations against the available experimental evidence⁸⁻⁹. We must decide first whether our structure for the crowded cavity after decarboxylation corresponds to

Table 2. Packing energy breakdown among fragments for the doubly decarboxylated TPPP molecule (Kcal/mole)^a.

	CO_2	T'	CO'_2	benzenes
T	-1.4	-0.3	-0.8	-4.5
CO_2	-	-0.8	+9.6	-0.7
T'		-	-1.4	-4.5
CO'_2			-	-0.7

^a) Lattice energy -106.3; total PPE -117.3; activation energy 18.1 Kcal/mole. Negative values are attractive. 10 Å cutoff.

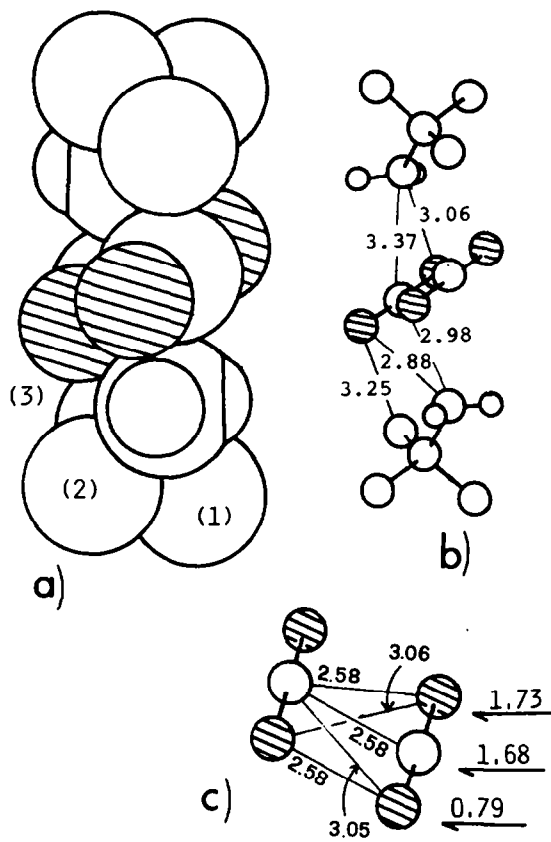


Figure 7. a) van der Waals envelopes of the final C_3CCH_2 and CO_2 groups (quaternary C omitted for clarity). b) and c) show non-bonded distances in the aggregate. Numbers on the arrows are total displacements of the COO group from the initial position. A units; dashed circles are oxygen atoms. See Figure 6 for the labels (1), (2), (3).

TT or TT*. Aside from small displacements of the CH_2 groups, which we cannot account for in a satisfactory manner, the main difference between the two is their reactivity towards neophyl rearrangement. TT* gives TR_1 , while the relaxed TT radical pair gives the topochemical product, TR_3 ⁹. Now, close scrutiny of Figure 7 (especially of the relevant non-bonded distances in Figure 7b) reveals that the CH_2 groups are wedged in between the two CO_2 molecules, and that each one of them is actually nearer to the CO_2 molecule detached from the other. It must therefore be quite easy for C(2) to slip past the obstacle of CO_2 and reach the carbon atom at ring 3, especially if, as it appears⁹, the C(2)-C(3) distance is shortened. The CO_2 molecules might help this process by small rotations in a direction perpendicular to the axis joining their C atoms (see Figure 7a). We may therefore assign our structure to the relaxed TT pair, which reacts to give TR_3 . TT* should be some intermediate in which the CH_2 groups are still under a strong push from their own CO_2 molecule; the barrier to TT*-TT relaxation (9.6 Kcal/mole⁸) may arise from some intermolecular obstacle encountered by CO_2 on its way along the 2 Å displacement to the stable structure (Figure 7c), or from some residual (intramolecular) bonding interaction between CH_2 and CO_2 .

The subtle motions of CH_2 after decarboxylation may be under the effect of intramolecular potentials (bond stretching and bond bending contributions) which are even more difficult to evaluate for a radical than for a neutral species. CH_2 has free space near it (Figure 6), but it may well be that it does not need it for its

motions. We have no ground at this point to discuss either intra- or intermolecular aspects of the neophyl rearrangements of T. Final product formation (Scheme II) requires radical pair collapse, and hence, motion of CO₂ molecules out of the way of the radicals that must meet each other. How this can happen is still unclear, but a major rearrangement in the reaction cage or in the surroundings is possible.

Conclusion

We believe we have successfully located the CO₂ molecules in the crowded cage after double decarboxylation of TPPP. Potential energy calculations and packing analysis are the only means to obtain this information. The reaction, which has a substantial volume of activation, has a relatively low intermolecular energy of activation. Our analysis reveals also that crystals with sizeable domains of reacted molecules could be obtained.

This study suggests that reactions of this kind in crystals with rather low packing coefficients may be easier than is usually thought. The maximum volume increment in such crystals could be estimated from the difference in the actual packing coefficient and the average one for each class of compounds¹³. Any molecular crystal with a packing coefficient below 0.7 and a potentially labile group, that could detach a small molecule, say CO₂, N₂, H₂O, Cl₂, NH₃, qualifies for such reactions in the solid state.

REFERENCES

- 1 M.D.Cohen and B.S.Green, *Chem. Brit.* 9,490 (1973).
- 2 I.C.Paul and D.Y.Curtin, *Acc. Chem. Res.* 6,217 (1973).
- 3 J.M.McBride, *Acc. Chem. Res.* 16,304 (1983).
- 4 J.R.Scheffer, *Acc. Chem. Res.* 13,283 (1980).
- 5 A.Gavezzotti and M.Simonetta, *Chem. Revs.* 82,1 (1982).
- 6 A.Gavezzotti and M.Simonetta, in: *Organic Solid State Chemistry*, G.R.Desiraju, Ed., Elsevier (in press).
- 7 A.I.Kitaigorodsky, *Molecular Crystals and Molecules*, Academic Press, New York 1973.
- 8 D.W.Walter and J.M.McBride, *J. Am. Chem. Soc.* 103,7069 (1981).
- 9 D.W.Walter and J.M.McBride, *J. Am. Chem. Soc.* 103,7074 (1981).
- 10 R.Bianchi and A.Gavezzotti, *Chem. Phys. Letters* 128,295 (1986).
- 11 A.Gavezzotti, *J. Am. Chem. Soc.* 105,5220 (1983).
- 12 A.Gavezzotti, *J. Am. Chem. Soc.* 107,962 (1985).
- 13 A.Gavezzotti, *Nouv. J. Chimie* 6,443 (1982).
- 14 R.Bianchi, A.Gavezzotti and M.Simonetta, *J. Mol. Struct. (TheoChem)* .135,391 (1986).
- 15 A.Gavezzotti and M.Simonetta, *Acta Cryst.* A31,645 (1975).
- 16 G.Filippini, A.Gavezzotti, M.Simonetta and R.Mason, *Nouv. J. Chimie* 5,211 (1981).
- 17 T.Beringhelli, G.Filippini, A.Gavezzotti and M.Simonetta, *J. Mol. Struct. (TheoChem)* 94,51 (1983).
- 18 R.K.Boyd, C.A.Fyfe and D.A.Wright, *J. Phys. Chem. Solids* 35,1355 (1974).
- 19 C.A.Fyfe and D.Harold-Smith, *J. Chem. Soc. Faraday II*, 967 (1975).
- 20 A.Gavezzotti and M.Simonetta, *Nouv. J. Chimie* 2,69 (1977).